the DMB ligand and its nucleotide loop can easily influence the chemical mechanism.

Acknowledgment. We thank Syed Khalid and Mike Sullivan for technical assistance at beamline X-9A. The construction and operation of beamline X-9A is supported by National Institute of Health Grant RR-01633, and National Science Foundation Grant DMR-85190959. The National Synchrotron Light Source at Brookhaven National Labs is supported by the Department of Energy, Division of Materials Science and Division of Chemical Science. This work is supported by the donors of the Petroleum Research Fund (administered by the American Chemical Society), a grant from the NRICGP-CSRS, U.S. Department of Agriculture, under agreement No. 91-37200-6180 of the Program in Human Nutrients, and a grant from the Upjohn Company.

Supplementary Material Available: Detailed description of the data analysis for aquocobalamin and cyanocobalamin, along with two data analysis tables and Fourier transforms of the background-subtracted data of cyanocobalamin and aquocobalamin (7 pages). Ordering information is given on any current masthead page.

A Stable Dinitrogen Complex of a Ruthenium Cofacial Diporphyrin

James P. Collman,* James E. Hutchison, Michel Angel Lopez,† and Roger Guilard†

Contribution from the Department of Chemistry, Stanford University, Stanford, California 94305-5080. *Received January 13, 1992*

Abstract: An unusually stable, bridged dinitrogen complex of a biphenylene bridged diporphyrin is described. The complex $(\mu\text{-}N_2)Ru_2DPB(1\text{-}tert\text{-butyl-}5\text{-phenylimidazole})_2$ (DPB = diporphyrinatobiphenylene tetraanion) is proposed as a model for a dinitrogen reduction catalyst based on cofacial metallodiporphyrins. The differences in binding by bridged and nonbridged ligands to the two coordination sites between the porphyrin rings are discussed. The complex's preparation, structural characterization, ligand substitution reactivity, electrochemistry, and acid–base properties are reported. It is proposed that the complex's unusual stability is due to a chelation of the dinitrogen by the two tethered metal centers. Loss of dinitrogen from the complex occurs only through replacement of dinitrogen by an added ligand. The rate of replacement is dependent on the concentration of the added ligand. Advantages of cofacial diporphyrins as dinitrogen electroreduction catalysts compared to monomeric or untethered binuclear dinitrogen complexes are noted.

The discovery of an electrode catalyst for the reduction of dinitrogen is a challenging and unsolved problem. The problem is interesting primarily from a fundamental rather than a technological point of view because the transformation of dinitrogen to ammonia by the Haber–Bosch process is fairly efficient and economically well-entrenched in spite of the high temperature and pressure required.[1]

The difficulty in reducing (or activating) dinitrogen derives from the strength of the N–N triple bond and the high ionization energy of dinitrogen. Over half the bond strength of the N–N bond (about 130 out of 225 kcal/mol)[2] is required to rupture the first π-bond. The first ionization potential of dinitrogen (15.6 eV)[2] rivals that of argon. The key to reducing nitrogen is to activate the LUMO's of N_2 with transition metals of the proper (low) d-electron configuration.

Even though dinitrogen is quite inert, its reduction to ammonia can be carried out at ambient temperature, atmospheric pressure, and neutral pH by the nitrogenase enzymes contained in anaerobic bacteria. Mo/Fe, V/Fe, and "Fe only" nitrogenase enzymes have been extensively studied,[3] and it is generally accepted that the site of dinitrogen reduction in these enzymes is at one or more of the metal centers. Although it has been shown that dinitrogen can be reduced stoichiometrically at a single metal center,[4] it is still unclear whether the binding sites of the enzymes include one or more metal atoms. A recent, low-resolution X-ray crystallographic study of the molybdoprotein of the *Clostridium pasteurianum* indicates that in the solid state the two molybdenum centers are 70 Å apart.[5] This evidence suggests that only one molybdenum center can be associated with each active site, but it does not preclude bridging complexes between molybdenum and iron, for example.

Chemists have tried for many years to develop systems that mimic the nitrogenase enzyme. The first chemical systems found to reduce dinitrogen were discovered by Vol'pin and Shur in the early 1960's. Similar systems involving early transition metals and strong reducing agents in ethereal solvents were developed independently by VanTamelen et al. These reduction systems involve forcing conditions, and little mechanistic information about them has been obtained. The work by both of these groups, including a report of a catalytic system, has been reviewed.[6]

Reports of catalytic reduction systems in aqueous solutions primarily include the work of Shilov or Schrauzer and involve either molybdenum or vanadium catalysts.[6a,7] These reduction systems are too complicated to allow elucidation of the mechanisms

† Present Address: Université de Bourgogne, Laboratorie de Synthèse et d' Electrosynthèse Organométallique Associé au C.N.R.S. (URA 33), Faculté des Sciences "Gabriel", 6, boulevard Gabriel, 21100 Dijon CEDEX, France.

(1) (a) Ertl, G. *Catal. Rev.* **1980**, *21*, 201–223. (b) Tamaru, K. In *Trends in the Chemistry of Nitrogen Fixation*; Chatt, J., da Câmara Piru, L. M., Richards, R. L., Eds.; Academic Press: New York, 1980; pp 17–70.

(2) Leigh, G. J. In *The Chemistry and Biochemistry of Dinitrogen Fixation*; Postgate, J. R., Ed.; Plenum Press: London, 1971; pp 19–56.

(3) (a) Postgate, J. R. *Nitrogen Fixation*; Edward Arnold Ltd.: London, 1987. (b) Burgess, B. K. *Chem. Rev.* **1990**, *90*, 1377–1406.

(4) Henderson, R. A. *Transition Met. Chem.* **1990**, *15*, 330–336 and references therein.

(5) Bolin, J. T.; Ronco, A. E.; Mortenson, L. E.; Morgan, T. V.; Williamson, M.; Xuaong, N.-h. In *Nitrogen Fixation: Achievements and Objectives. Proceedings of the 8th International Congress on Nitrogen Fixation*; Gresshoff, P. M., Roth, L. E., Stacey, G., Newton, W. E., Eds.; Chapman and Hall: New York, 1990; pp 117–124.

(6) (a) Dilworth, J. R.; Richards, R. L. In *Comprehensive Organometallic Chemistry*; Wilkinson, G., Ed.; Pergamon Press: Oxford, 1982; Vol. 8, pp 1073–1106. (b) Van Tamelen, E. E. *Acc. Chem. Res.* **1970**, *3*, 361–367. (c) Van Tamelen, E. E.; Seeley, D. A. *J. Am. Chem. Soc.* **1969**, *91*, 5194.

(7) Shilov, A. E. In *Energy Resources through Photochemistry and Catalysis*; Academic Press: New York, 1983; Chapter 16, pp 535–558.

0002-7863/92/1514-8066$03.00/0

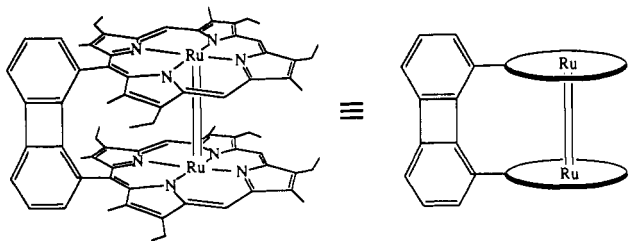

Figure 1. Structure of the metal–metal bonded biphenylene bridged diporphyrin, Ru_2DPB.

by which they operate: this is unfortunate in light of the catalytic activity demonstrated.

Perhaps the most successful designed dinitrogen reduction systems are those pioneered by Chatt and co-workers. Treatment of *cis*- or *trans*-$(N_2)_2W(PPhMe_2)_4$ with excess acid produces nearly 2 mol of ammonia per tungsten center: the other bound dinitrogen is liberated and the complex is completely degraded.[8] Stoichiometric protonation of an analogous dinitrogen complex *trans*-$(N_2)_2W(Ph_2PCH_2CH_2PPh_2)_2$ followed by electrochemical reduction (Hg electrode, THF, −2.6 V vs $FeCp_2^{+/0}$) of the resulting hydrazido complex yields ammonia (0.22–0.24 mol per mol of hydrazido complex) and a trace of hydrazine (0.01–0.02 mol per mol of hydrazido complex) and regenerates nearly all of the starting dinitrogen complex (85–95% recovery).[9] The dinitrogen complex can be stoichiometrically protonated again and electroreduced to yield additional ammonia. This cycle could, in theory, be repeated many times. The yield of ammonia after three cycles is 0.73 NH_3/W center. The mechanism of dinitrogen reduction in this system has been thoroughly discussed in the literature.[10]

A bridged dinitrogen complex $[Mo(C_5Me_5)Me_3](\mu\text{-}N_2)[W(C_5Me_4Et)Me_3]$ synthesized in Schrock's lab yields up to 1.86 equiv of ammonia per dinitrogen complex when protonated in the presence of zinc amalgam.[11] However, the analogous homobimetallic complexes (Mo/Mo and W/W) liberate only about half as much ammonia under identical conditions. The possibility of developing a dinitrogen reduction catalyst involving bridged dinitrogen complexes of high-valent Mo or W fragments is complicated by the fact that it is not possible to rule out decomposition of the bimetallic complex to the monomeric tungsten hydrazido complex which is known to liberate nearly 2 equiv of ammonia under similar reaction conditions.

Recently, another bridged dinitrogen complex $[\{V(C_6H_4CH_2NMe_2)_2(C_5H_5N)\}_2(\mu\text{-}N_2)]$ has been shown to produce some ammonia (33%) upon protonation. Thus far, the fate of the metal centers has not been reported.[12]

Our approach to developing a dinitrogen electrode catalyst[13-15] is also based on bridged dinitrogen complexes. This approach utilizes cofacial metalloporphyrins and is thus analogous to our application of cofacial bis-cobalt diporphyrins as electrode catalysts for the four-electron reduction of dioxygen.[16] By extending the results of molecular orbital analyses[17] of bridging dinitrogen between two idealized transition metal centers to cofacial metallodiporphyrins we can predict which metallocofacial diporphyrins should activate dinitrogen. The best heterobimetallic cofacial metalloporphyrin catalysts for the electroreduction of dinitrogen should be those that contain a dinitrogen binding center, Ru(II) or Os(II) for example, and a Lewis acid such as Al(III) or Ti(IV). Homobimetallic systems involving metals where the overall d-electron count for the two metals is between 4 and 8, Mo(II) and V(II) for example, should also activate dinitrogen. Because the heterobimetallic systems are difficult to synthesize and the early transition metal complexes of porphyrins tend to be quite oxygen- and water-sensitive, we initially chose a more convenient system, Ru^{II}/Ru^{II}(cofacial diporphyrin), as a starting point even though such a complex is not expected to activate dinitrogen.

In our early studies we found that neither the diruthenium cofacial diporphyrin, Ru_2DPB[18] (Figure 1), nor the bis(triphenylphosphine) ruthenium cofacial diporphyrin, $Ru_2DPB(PPh_3)_2$, reacts with dinitrogen.[15] More recently we reported that a cofacial diruthenium diporphyrin with imidazoles as exterior axial ligands forms a stable bridged dinitrogen complex.[19] In this paper we describe the synthesis and structural characterization of this dinitrogen complex as well as its redox, acid/base, and ligand-exchange properties. These studies are the foundation for future mechanistic and synthetic studies involving the unusual coordination environment between the cofacial diporphyrins. The second of this pair of papers shows the utility of this unique coordination environment for effecting redox transformations between reduced nitrogen hydride substrates.[20]

Results

Synthesis and Reactivity of a Bis(five-coordinate) Ruthenium Cofacial Diporphyrin. Treatment of the cofacial dimer Ru_2DPB[15] with 2 equiv of 1-*tert*-butyl-5-phenylimidazole, *Im, in benzene under argon initially yields a bis(five-coordinate) complex, $Ru_2DPB(*Im)_2$ (eq 1). In solution this bis(five-coordinate)

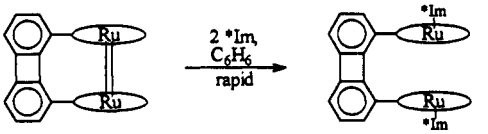

(1)

complex is unstable with respect to disproportionation and after several hours a 50:50 mixture of Ru_2DPB and a bis(six-coordinate) complex, $Ru_2DPB(*Im)_4$, results (eq 2). The ^1H NMR spectrum

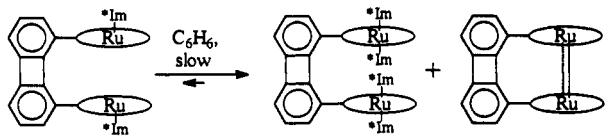

(2)

of $Ru_2DPB(*Im)_4$ displays one set of porphyrin signals (suggesting that the metal in each ring has the same axial substitution) and

(8) Chatt, J.; Pearman, A. J.; Richards, R. L. *Nature* **1975**, *253*, 39–40.
(9) Pickett, C. J.; Talarmin, J. *Nature* **1985**, *317*, 652–653.
(10) Pickett, C. J.; Ryder, K. S.; Talarmin, J. *J. Chem. Soc., Dalton Trans.* **1986**, 1453–1457.
(11) Schrock, R. R.; Kolodziej, R. M.; Liu, A. H.; Davis, W. M.; Vale, M. G. *J. Am. Chem. Soc.* **1990**, *112*, 4338–4345.
(12) Leigh, G. J.; Prieto-Alcón, R.; Sanders, J. R. *J. Chem. Soc., Chem. Commun.* **1991**, 921–922.
(13) Collman, J. P.; Elliot, C. M.; Halbert, T. R.; Tovrog, B. S. *Proc. Natl. Acad. Sci. U.S.A.* **1977**, *74*, 18–22.
(14) Kim, K. Ph.D. Thesis, Stanford University, 1986.
(15) Collman, J. P.; Kim, K.; Leidner, C. R. *Inorg. Chem.* **1987**, *26*, 1152–1157.
(16) Collman, J. P.; Denisevich, P.; Konai, Y.; Marrocco, M.; Koval, C.; Anson, F. C. *J. Am. Chem. Soc.* **1980**, *102*, 6027–6036.
(17) (a) Treitel, I. M.; Flood, M. T.; Marsh, R. E.; Gray, H. B. *J. Am. Chem. Soc.* **1969**, *91*, 6512–6513. (b) Chatt, J.; Fay, R. C.; Richards, R. L. *J. Chem. Soc. A* **1971**, 702–704. (c) Chatt, J.; Richards, R. L. In *The Chemistry and Biochemistry of Nitrogen Fixation*; Postgate, J. R., Ed.; Plenum: London, 1971; pp 57–103. (d) Powell, C. B.; Hall, M. B. *Inorg. Chem.* **1984**, *23*, 4619–4627.

(18) Abbreviations: DPB = diporphyrinatobiphenylene tetraanion, *Im = 1-*tert*-butyl-5-phenylimidazole; TMP = *meso*-tetramesitylporphyrinato dianion; OEP = octaethylporphyrinato dianion; pyr = pyridine; THF = tetrahydrofuran; NHE = normal hydrogen electrode; $FeCp_2$ = ferrocene; CPK = Corey–Pauling–Koltun space filling models.
(19) Collman, J. P.; Hutchison, J. E.; Lopez, M. A.; Guilard, R.; Reed, R. A. *J. Am. Chem. Soc.* **1991**, *113*, 2794–2796.
(20) The following paper in this issue.
(21) Weatherburn, M. W. *Anal. Chem.* **1967**, *39*, 971–974.
(22) Watt, G. W.; Chrisp, J. D. *Anal. Chem.* **1952**, *24*, 2006–2008.
(23) Fillers, J. P.; Ravichandran, K. G.; Abdalmuhdi, I.; Tulinsky, A.; Chang, C. K. *J. Am. Chem. Soc.* **1986**, *108*, 417–424.
(24) Slip angle = $\sin^{-1}$ [(magnitude of slip)/(metal–metal distance)].[23]
(25) (a) James, B. R.; Mikkelsen, S. R.; Leung, T. W.; Williams, G. M.; Wong, R. *Inorg. Chim. Acta* **1984**, *85*, 209–213. (b) Sishta, C.; Camenzind, M. J.; James, B. R.; Dolphin, D. *Inorg. Chem.* **1987**, *26*, 1181–1182. (c) Collman, J. P.; Brauman, J. I.; Fitzgerald, J. P.; Sparapany, J. W.; Ibers, J. A. *J. Am. Chem. Soc.* **1988**, *110*, 3486–3495. (d) Collman, J. P.; Venberg, G. D. Manuscript in preparation.

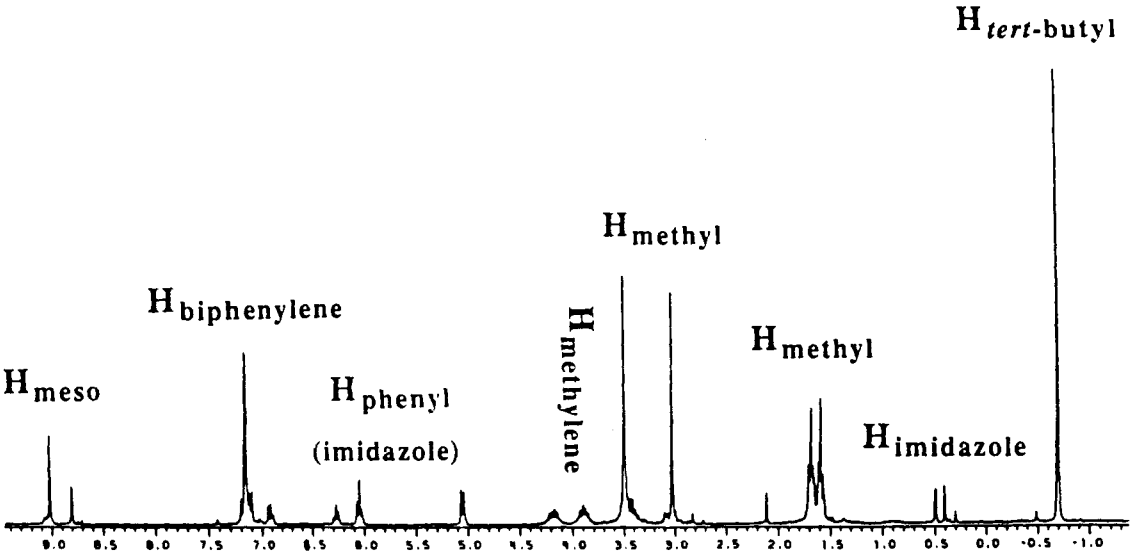

Figure 2. The proton NMR spectrum of the dinitrogen complex $(\mu\text{-}N_2)Ru_2DPB(*Im)_2$ in benzene-d_6.

has two inequivalent *tert*-butyl signals which each integrate to 18 protons relative to the diporphyrin. This bis(six-coordinate) complex also displays the expected molecular ion in the mass spectrum. Efforts to "shut off" this disproportionation with bulkier axial ligands that we thought could not gain access to the interior coordination sites (4-tritylpyridine, *N*-tritylimidazole, and 1,5-dicyclohexylimidazole) failed. When used in excess, each of these ligands bound to both the exterior and interior coordination sites of the cofacial diporphyrin. Addition of 4 equiv of *Im to the dimer causes immediate rupture of the metal–metal bond (as the imidazoles coordinate to the outside of the porphyrin cavity) followed by a slower reaction involving coordination of the second 2 equiv of *Im to the interior sites (eq 3).

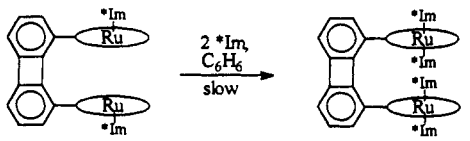

Synthesis and Characterization of the Dinitrogen Complex. Addition of 2 equiv of *Im to a benzene solution of the metal–metal bonded diruthenium cofacial diporphyrin, Ru_2DPB, under a dinitrogen atmosphere rapidly produces $(\mu\text{-}N_2)Ru_2DPB(*Im)_2$ in quantitative yield (eq 4). The same reaction using ^{15}N-labeled

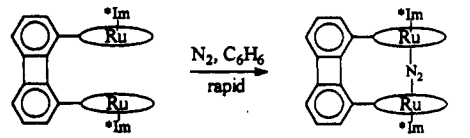

dinitrogen yields $(\mu\text{-}^{15}N_2)Ru_2DPB(*Im)_2$. Alternatively, the dinitrogen complex is prepared by exposing a benzene solution of either (1) the dihydrogen complex, $(\mu\text{-}H_2)Ru_2DPB(*Im)_2$[26] (eq 5), or (2) a 50:50 mixture of the dimer, Ru_2DPB, and the bis-

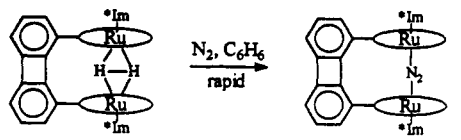

(six-coordinate) complex, $Ru_2DPB(*Im)_4$ (eqs 2 and 4), to an atmosphere of dinitrogen. Recrystallization from dichloromethane/methanol yields analytically pure $(\mu\text{-}N_2)Ru_2DPB(*Im)_2$.

^1H NMR (Figure 2) of $(\mu\text{-}N_2)Ru_2DPB(*Im)_2$ in benzene-d_6 shows that the two porphyrin rings are equivalent and that there is a pair of equivalent axial imidazoles bound to the complex. $(\mu\text{-}N_2)Ru_2DPB(*Im)_2$ displays the expected molecular ion cluster in the mass spectrum. ^{15}N NMR of $(\mu\text{-}^{15}N_2)Ru_2DPB(*Im)_2$ displays a singlet (at 108 ppm upfield of (^{15}N)-nitrobenzene). Because no ^{15}N NMR data are available for dinitrogen complexes of ruthenium porphyrins, we measured the spectrum of $(^{15}N_2)$-Ru(THF)TMP. In toluene-d_8 at −30 °C, two broad signals are observed at −61 and −96 ppm versus (^{15}N)-nitrobenzene.

The IR spectrum of $(\mu\text{-}N_2)Ru_2DPB(*Im)_2$ exhibits no absorptions corresponding to ν(N–N). Raman spectra of $(\mu\text{-}N_2)$-$Ru_2DPB(*Im)_2$ were collected at a variety of excitation wavelengths (406.7, 413.13, 441.6, 457.9, 488.0, 514.5, 520.8, and 530.8 nm). The best ν(N–N) stretch data were obtained using 413.13-nm excitation. The dinitrogen stretch is observed at 2112 cm^{-1} for the ^{14}N derivative and shifts down to 2042 cm^{-1} upon ^{15}N substitution. The observed downshift (70 cm^{-1}) agrees well with the value calculated (69 cm^{-1}) on the basis of a simple harmonic oscillator.

Replacement of Dinitrogen with Added Axial Ligands. There is no measurable loss of dinitrogen (as determined by ^1H NMR) from $(\mu\text{-}N_2)Ru_2DPB(*Im)_2$ during five cycles of freeze–pump–thaw. Furthermore, $(\mu\text{-}N_2)Ru_2DPB(*Im)_2$ is air-stable indefinitely in the solid state and for hours in solution. In the presence of potential axial ligands such as pyridine or carbon monoxide, the dinitrogen ligand is slowly replaced.

The product of ligand replacement by pyridine was identified as $Ru_2DPB(*Im)_2(pyr\text{-}inside)_2$ by dissolving the dinitrogen complex in pyridine-d_5 and following the reaction by ^1H NMR at 60 °C. Within an hour, the resonances due to the dinitrogen complex had been replaced by new signals which correspond to a new species which still has equivalent porphyrin rings and retains the bound imidazoles. Over a period of several more hours at 60 °C replacement of the outer axial imidazoles to form the known compound $Ru_2DPB(pyr)_4$[15] was not observed. Treatment of the dinitrogen complex with pyridine for several days at room temperature followed by removal of the solvent gave $Ru_2DPB(*Im)_2(pyr\text{-}inside)_2$ in quantitative yield. ^1H NMR in benzene-d_6 shows one set of resonances corresponding to the two equivalent pyridines bound between the porphyrin rings in addition to the porphyrinic and imidazole resonances observed for $Ru_2DPB(*Im)_2(pyr\text{-}d_5\text{-}inside)_2$.

Preliminary UV/vis experiments in benzene showed that the dinitrogen complex is cleanly converted to $Ru_2DPB(*Im)_2(pyr\text{-}inside)_2$ at 60 °C on the basis of good isosbestic points at 381 and 537 nm (Figure 3). The rates of the reaction were determined by following the increase in absorbance at 528 nm in toluene/pyridine solutions over a range of pyridine concentrations (0.44–12.21 M). Small changes in absorbance of $(\mu\text{-}N_2)$-$Ru_2DPB(*Im)_2$ and $Ru_2DPB(*Im)_2(pyr\text{-}inside)_2$ as a function of

(26) Collman, J. P.; Hutchison, J. E.; Wagenknecht, P. S.; Lewis, N. S.; Lopez, M. A.; Guilard, R. *J. Am. Chem. Soc.* **1990**, *112*, 8206–8208.

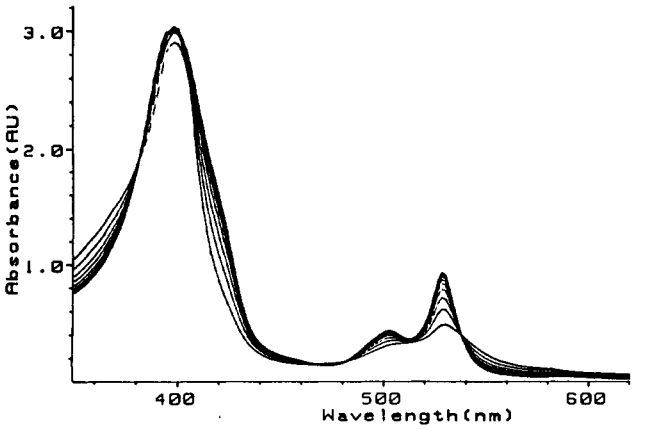

Figure 3. Plot showing the replacement of the dinitrogen ligand of $(\mu\text{-}N_2)Ru_2DPB(*Im)_2$ by pyridine at 60 °C. [Dinitrogen complex]$_i$ = 1.69×10^{-5} M. [pyridine] = 8.83 M. Time interval between scans is 120 s.

pyridine concentration and temperature precluded obtaining accurate extinction coefficients for the two species. To circumvent this problem, plots of absorbance vs time were curve fit using nonlinear least-squares analysis to obtain the observed rate constants (k_{obs}).

Although these experiments were done under a dinitrogen atmosphere, control experiments performed under argon in argon-saturated toluene showed that the rate is not different under those conditions. At 60 °C in the absence of pyridine, the absorbance over the entire spectrum *decreases*. This seems to be caused by deposition of the dinitrogen complex on the walls of the cell above the surface of the solution. The decrease is small even for long reaction times and likely does not significantly affect the absorbance vs time data during the time frame of the kinetic runs.

Electrochemistry of the Dinitrogen Complex. The cyclic voltammograms of the dinitrogen complex in dichloromethane containing 0.2 M tetra-*n*-butylammonium hexafluorophosphate are shown in Figure 4. Each observable wave during the positive scan is an oxidation as determined by rotating disk voltammetry. There are no reduction waves within the solvent breakdown limit. The first oxidation of the dinitrogen complex occurs at +0.03 V vs NHE, is reversible, and presumably leads to the mixed-valence complex, $[(\mu\text{-}N_2)Ru_2^{II/III}DPB(*Im)_2]^+$ (based on the potential compared to other metal-based and ring-based oxidations[15]). The next oxidation wave (E_{pa} = +0.73 V vs NHE) is irreversible (i_{pc}/i_{pa} = 0.29 at 500 mV/s). This wave likely involves oxidation to the dication, $[(\mu\text{-}N_2)Ru_2^{III/III}DPB(*Im)_2]^{2+}$, which rapidly loses dinitrogen. On the reverse scan, two new irreversible waves (E_{pc} = +0.19 and −0.61 V) are observed which correspond to the reduction of the $[Ru_2^{III/III}DPB(*Im)_2]^{2+}$ complex. During successive scans, the peak currents for the oxidation waves of the dinitrogen complex are diminished compared to the first scan; however, holding the potential at −0.70 V for 30 s before scanning positive again regenerates the initial voltammogram.

Attempted Reductions and Protonations of the Dinitrogen Complex. Treating a benzene solution of the dinitrogen complex with sodium amalgam for several days resulted in no reaction. Addition of 2 equiv of trifluoroacetic acid to a benzene-d_6 solution of the dinitrogen complex resulted in broadening of all the complex's resonances in the ^1H NMR spectrum. Stirring this solution over solid sodium methoxide for 30 min regenerated the dinitrogen complex suggesting that the reaction with the acid is reversible. Stirring the acid-treated dinitrogen complex with several chunks of zinc amalgam overnight yields mostly unreacted dinitrogen complex and uncharacterized porphyrinic products. Treatment of the red dinitrogen complex with more than 100 equiv of acid and excess zinc amalgam gave an insoluble brown solid after the solution was stirred overnight. In another trial, 50 equiv of acid and an excess of zinc amalgam were used and the mixture was analyzed for ammonia[21] and hydrazine.[22] Neither of these dinitrogen reduction products were detected under the reduction conditions.

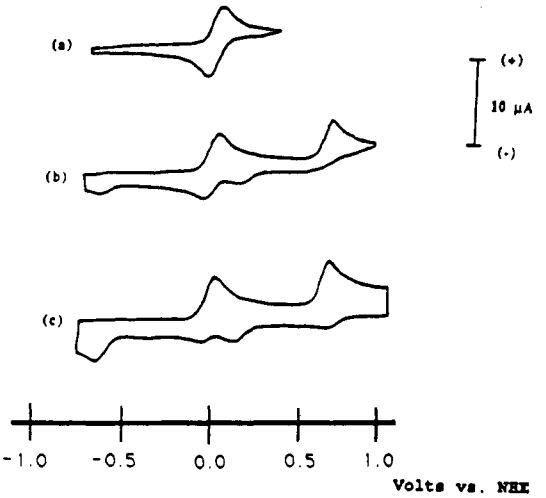

Figure 4. Cyclic voltammograms of $(\mu\text{-}N_2)Ru_2DPB(*Im)_2$ vs NHE in 0.2 M tetra-*n*-butylammonium hexafluorophosphate/dichloromethane at 100 mV/s. Scan (a) was reversed after passing through the first anodic wave. Scan (b) was reversed after the second anodic wave. Scan (c) was held for 1 min at +1.05 V (after passing through the first two anodic waves) before the reverse scan was finished.

Discussion

The Coordination Environment between the Cofacial Diporphyrins. It is important to consider the steric constraints of the cofacial diporphyrin because the space between the porphyrin rings is an unusual coordination environment. The steric confines of the diporphyrin are different for a bridging ligand than for a terminal ligand. The binding orientation for a bridging ligand is controlled by the distance between the two metal centers whereas binding of terminal ligands is largely affected by contact between the ligand and the opposing porphyrin ring.

Because of the rigid biphenylene spacer, the metal centers remain approximately 3.8 Å apart[23] independent of the slip angle,[24] the angle between the plane containing the porphyrin ring and the plane containing the biphenylene spacer. Any deviation from the normal metal–metal distance will require doming or splaying of the porphyrin rings (vide infra). For a bridging ligand such as dinitrogen, the binding cavity is constraining and we expect that a bridged dinitrogen complex of a metallo-DPB derivative will have a strained structure.

The cavity of the cofacial diporphyrin is crowded for terminal ligands as well, but not to the degree that one might suspect. A CPK model of a typical metallo-DPB complex suggests that bulky ligands such as the imidazole (*Im) are too large to coordinate to the interior coordination sites. Consequently we were initially surprised to find that the bulky ligands bind to the interior sites. Because the diporphyrin is only singly bridged it is somewhat floppy, thus the two porphyrin rings might flex and twist to allow bulky ligands to avoid steric interactions perhaps as is shown in Figure 5.

Synthesis and Reactivity of $Ru_2DPB(*Im)_2$ under Argon. The reaction of the metal–metal bonded dimer with 1-*tert*-butyl-5-phenylimidazole presumably proceeds by *Im attacking the open (outside) coordination sites of the ruthenium centers and thus breaking the metal–metal bonds. This type of bond cleavage is consistent with the fact that initial reaction of the dimer with *Im and the subsequent reaction at the inside coordination sites by small ligands are very fast whereas reaction by additional *Im at the inside sites is much slower.

After several hours, however, 4 equiv of *Im bind to all of the available coordination sites. Over the same time frame in the absence of additional axial ligand, the bis(five-coordinate) complex, under argon, disproportionates to a 50:50 mixture of $Ru_2DPB(*Im)_4$ and Ru_2DPB (eq 2). These two species must be in equilibrium with a small amount of the bis(five-coordinate)

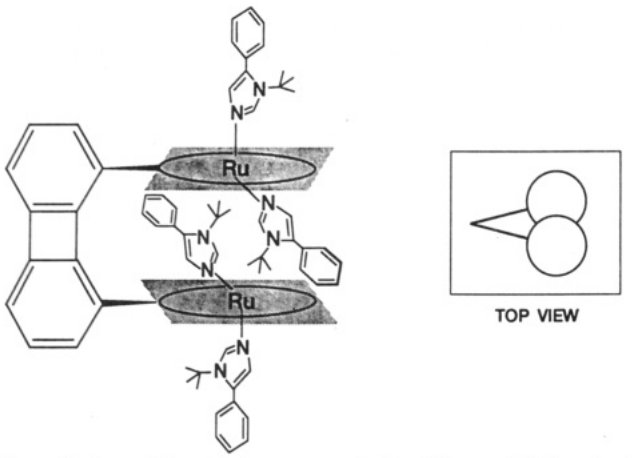

Figure 5. A possible mode for accommodation of large axial ligands at the inside coordination sites of the cofacial metallodiporphyrin, M_2DPB.

complex because treatment of the mixture with dinitrogen slowly produces the dinitrogen complex yet neither the dimer nor the bis(six-coordinate) complex reacts with dinitrogen.

What is the nature of the driving force for this disproportionation? It is clear that the bis(five-coordinate) complex $Ru_2DPB(*Im)_2$ is the kinetic product, whereas the 50:50 mixture is the thermodynamically favored state. The instability of 5-coordinate Ru(porphyrin) complexes involving a nitrogenous axial ligand has been observed before.[25] The only stable complex is the 5-coordinate Ru("picnic basket" porphyrin)(1,5-dicyclohexylimidazole) where binding by large ligands is strictly prohibited on one face of the porphyrin.[25c] The ^1H NMR of the 5-coordinate "picnic basket" porphyrin is quite broadened, suggesting that the compound is paramagnetic and may be high spin. Because the 6-coordinate complexes are low spin, it may be that the driving force for the disproportionation in the cofacial system is a high-to-low spin change. Five-coordinate Ru[porphyrin]-phosphine complexes are low spin and have no tendancy to undergo disproportionation. Regardless of the driving force, coordination to the interior sites of the cofacial diporphyrin likely requires significant distortion of the cofacial diporphyrin's geometry, and these steric effects slow down coordination to the inside sites and as a result slow down, but do not stop, the disproportionation.

Reactions of $Ru_2DPB(*Im)_2$ with Dinitrogen and Dihydrogen: Structure of the Dinitrogen Complex. The bis(five-coordinate) complex $Ru_2DPB(*Im)_2$ is much more reactive than its bis(triphenylphosphine) analog $Ru_2DPB(PPh_3)_2$.[15] The bis(1-*tert*-butyl-5-phenylimidazole) complex $Ru_2DPB(*Im)_2$ reacts rapidly with dinitrogen to produce a bridged complex. When prepared under a dihydrogen atmosphere, $Ru_2DPB(*Im)_2$ readily binds dihydrogen.[26] The geometry of the bridged dihydrogen ligand of the dihydrogen complex in solution has recently been determined to be an unusual bridged side-on/side-on species by high-field NMR studies.[27] As previously noted, the dihydrogen ligand in this complex is easily replaced by dinitrogen.

The composition of $(\mu\text{-}N_2)Ru_2DPB(*Im)_2$ and the bridging nature of the dinitrogen ligand are confirmed by ^1H NMR, ^{15}N NMR, mass spectroscopy, and Raman spectroscopy. The ^1H NMR spectrum reveals the equivalence of the two porphyrin rings and the ratio of 2:1 of axial imidazoles to cofacial diporphyrin. The molecular ion in the mass spectrum lead us to believe that the complex contained one bridging dinitrogen ligand although we could not at that time dismiss the possibility that a bis(dinitrogen) complex $(N_2\text{-inside})_2Ru_2DPB(*Im)_2$ might give "$(N_2)Ru_2DPB(*Im)_2$" as the highest molecular weight fragment. The bridging formulation was subsequently verified by application of ^{15}N NMR: The observed singlet is consistent with a single

Table I. ^{15}N NMR Data for Terminal and Bridging Dinitrogen Complexes of Ruthenium

compd	N_α	N_β	solvent	ref
$[(^{15}N_2)Ru(NH_3)_5]Br_2$	−81.3[a]	−43.8[a]	10^{-3} M HCl	28
$(^{15}N_2)Ru(TMP)(THF)$	−96[c] (−88)[d]	−61[c] (−53)[d]	toluene	*b*
$[(^{15}N_2)\{Ru(NH_3)_5\}_2](BF_4)_4$	+209.1[a]		water[a]	29
$(^{15}N_2)Ru_2DPB(*Im)_2$	+108[c] (+116)[d]		toluene	*b*

[a] Shifts relative to $^{15}N\text{-}CH_3NO_2$. [b] This work. [c] Shifts relative to $^{15}N\text{-}C_6H_5NO_2$. [d] Shift converted vs $^{15}N\text{-}CH_3NO_2$. The resonance for nitrobenzene is 8 ppm downfield of nitromethane.

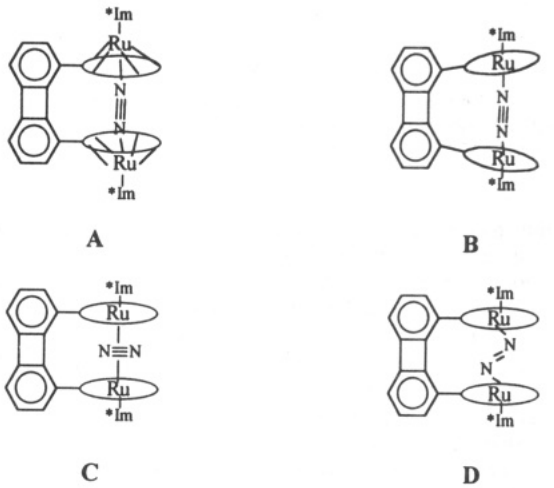

Figure 6. Possible binding modes for the bridged dinitrogen ligand.

bridged dinitrogen ligand. The ^{15}N NMR data for the bridged compound and a terminal dinitrogen complex of a metalloporphyrin $(N_2)Ru(TMP)(THF)$ are compared to data for non-porphyrinic analogs in Table I. Once the upfield shifts caused by the porphyrin ring currents are taken into account, the chemical shifts of the porphyrinic and non-porphyrinic complexes are comparable. The large magnitude of the down field shift of the signals for the bridged structures has been attributed to electronic effects.[29] Our interpretation of the ^{15}N NMR data led us to believe that the bridged dinitrogen ligand in $(\mu\text{-}N_2)Ru_2DPB(*Im)_2$ is similar to that in $[(NH_3)_5RuNNRu(NH_3)_5]^{4+}$.

The value of 2112 cm^{-1} for ν(N–N) for $(\mu\text{-}N_2)Ru_2DPB(*Im)_2$ is in the normally observed range for linear ruthenium porphyrin dinitrogen complexes (2060–2150 cm^{-1}).[30] More specifically, it is very close to the value of 2100 cm^{-1} obtained for $[(NH_3)_5RuNNRu(NH_3)_5]^{4+}$.[31] Again, from the value of ν(N–N) we believe that there is nothing unusual about the coordination of the dinitrogen ligand.

Because the dinitrogen ligand appears to be ordinary by spectroscopic techniques but is bound in what must be a constrained coordination environment, the binding geometry of the dinitrogen ligand is of particular interest. Although crystals have been grown (from several different solvent combinations) for X-ray diffraction, thus far we have not successfully determined the structure of the complex. Data from a partially refined[32] structure are consistent with a dinitrogen bridge which is nearly linear and

(27) Collman, J. P.; Wagenknecht, P. S.; Hutchison, J. E.; Lewis, N. S.; Lopez, M. A.; Guilard, R.; L'Her, M.; Bothner-By, A. A.; Mishra, P. K. *J. Am. Chem. Soc.* **1992**, *114*, 5654–5664.

(28) Donovan-Mtunzi, S.; Richards, R. L.; Mason, J. *J. Chem. Soc., Dalton Trans.* **1984**, 469–474.

(29) Donovan-Mtunzi, S.; Richards, R. L.; Mason, J. *J. Chem. Soc., Dalton Trans.* **1984**, 2429–2433.

(30) (a) James, B. R.; Addison, A. W.; Cairns, M.; Dolphin, D.; Farrell, N. P.; Paulson, D. R.; Walker, S. In *Fundamental Research in Homogeneous Catalysis*; Tsutsui, M., Ed.; Plenum: New York, 1979; Vol. 3, pp 751–772. (b) Camenzind, M. J.; James, B. R.; Dolphin, D. *J. Chem. Soc., Chem. Commun.* **1986**, 1137–1139. (c) Camenzind, M. J.; James, B. R.; Dolphin, D.; Sparapany, J. W.; Ibers, J. A. *Inorg. Chem.* **1988**, *27*, 3054–3057. (d) Reference 25c, this work.

(31) Chatt, J.; Nikolsky, A. B.; Richards, R. L.; Sanders, J. R. *Chem. Commun.* **1969**, 154–155.

(32) Collman, J. P.; Hutchison, J. E.; Ibers, J. A. Unpublished results. A partially refined structure suggests Ru–Ru ≈ 4.85 Å, Ru–N ≈ 1.9 Å, N–N ≈ 1.1 Å, Ru–N–N ≈ 170°.

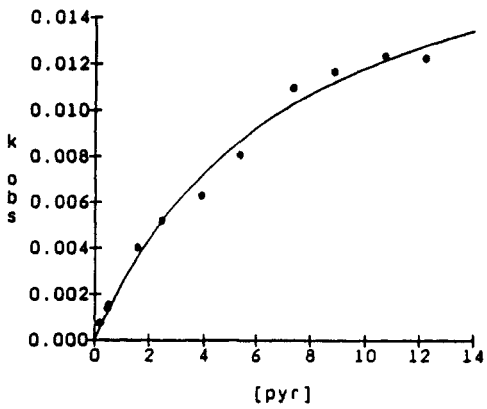

Figure 7. Plot showing the dependence of the observed rate constant for dinitrogen replacement from $(\mu\text{-}N_2)Ru_2DPB(*Im)_2$ on the concentration of pyridine (k_{obs} in s^{-1}, [pyridine] in M). The line is a curve fit to the data based on the analysis presented in the discussion.

has Ru–N and N–N bond lengths similar to those for $(NH_3)_5RuNNRu(NH_3)_5$.[17a] Given the spectroscopic data and the geometric constraints of the cofacial diporphyrin, several binding geometries can be proposed (Figure 6). Two of these involve distortions of the cofacial metallodiporphyrin, whereas the other two involve deviation from a linear binding geometry for the dinitrogen ligand. The proposed structures involve doming of the porphyrin ligand (A), flaring out of the diporphyrin's rings (B), and slight bending of the Ru–N–N angles (D). The preliminary X-ray data do not support a structure such as C. Doming of the porphyrin rings has been observed in several crystal structures of porphyrins including the dimer $[Ru(OEP)]_2$ (each Ru atom is 0.30 Å out of plane)[33] and the CoAl(OR)DPB complex (the Al atom is 0.365 Å out of plane).[34] The actual structure probably takes up the strain through slight distortions in each of the modes shown in A, B, and D.

Stability of the Dinitrogen Complex and the Mechanism of Dinitrogen Replacement. Compared to terminal dinitrogen complexes of metalloporphyrins, $(\mu\text{-}N_2)Ru_2DPB(*Im)_2$ is unusually stable toward the loss of dinitrogen. Terminal dinitrogen complexes of ruthenium porphyrins liberate dinitrogen readily upon degassing,[30] yet the dinitrogen ligand in $(\mu\text{-}N_2)Ru_2DPB(*Im)_2$ remains intact through many cycles of freeze–pump–thaw.

Although the dinitrogen ligand in $(\mu\text{-}N_2)Ru_2DPB(*Im)_2$ can be replaced by incoming ligands to form complexes containing two ligands in place of dinitrogen, this reaction is much slower than the analogous replacement involving terminal dinitrogen complexes of ruthenium porphyrins.[30] The mechanism of dinitrogen ligand replacement may shed light on the origin of the unusual stability of the dinitrogen complex.

The first-order dependence of the rate of dinitrogen replacement on the concentration $(\mu\text{-}N_2)Ru_2DPB(*Im)_2$ in the presence of excess pyridine is verified by the fact that plots of the exponentially increasing absorbance (at 528 nm) vs time give good nonlinear least-squares fits. The rate of replacement is dependent on the concentration of the incoming ligand, pyridine. The data of k_{obs} vs [pyridine] are graphically shown in Figure 7. The dependence of the observed rate constants on pyridine concentration is nonlinear. A log–log plot of these data is also nonlinear.

Based on the fact that the pyridine concentration dependence appears to be closer to first order at low concentrations, but closer to zero-order at higher pyridine concentrations, we propose the mechanistic scheme shown in Figure 8. In the first step in the replacement reaction, one of the dinitrogen–ruthenium bonds ruptures to form the unstable intermediate (**6**). Reformation of this bond should be extremely rapid. In the second step pyridine reacts with the vacant coordination site to form **7**. Once pyridine is bound, the dinitrogen ligand in **7** is extremely labile by analogy to monomeric ruthenium porphyrin dinitrogen complexes. The ligand association to convert **8** to **5** should be rapid as well. Therefore, the rate-limiting step is either the first or second step depending on the pyridine concentration.

The rate law for the reaction, assuming a steady-state concentration of **6**, is given in eq 6.

$$-(d[(4)]/dt)/([(4)]) = k_1k_2[\text{pyridine}]/(k_{-1} + k_2[\text{pyridine}]) \quad (6)$$

The curve drawn through the points in Figure 7 is a fit to the data of eq 6 using nonlinear least-squares analysis. The correlation coefficient is 0.997. The computer fit gives values for k_1 ($\cong$0.02 s^{-1}), k_{-1} ($\cong$5 s^{-1}), and k_2 ($\cong$0.7 M^{-1} s^{-1}); however, we do not have enough data points to minimize the error in these values.

These rough numbers fit well with the proposed mechanism. The intramolecular recoordination of dinitrogen (k_{-1}) should be fast compared to the dissociation of the first dinitrogen–metal bond (k_1). The proposed mechanism accounts for the fact that at higher pyridine concentrations the rate of the reaction slows as the bimolecular conversion from **6** to **7** begins to compete with the conversion of **6** back to **4**.

The stability of this bridged dinitrogen complex derives from the fact that the two ruthenium centers are held in place by the rigid biphenylene linker allowing the two metal centers to "chelate" dinitrogen. This is an unusual example of "host–guest" chemistry and has not, to our knowledge, been previously demonstrated for dinitrogen. Although dinitrogen commonly forms bridged complexes between two otherwise unconnected transition metal centers, this is the first case where two tethered metal centers act jointly to bind dinitrogen.

Electrochemical and Acid/Base Properties of the Dinitrogen Complex. Oxidation of the dinitrogen complex initially yields the cation $[(\mu\text{-}N_2)Ru_2^{II/III}DPB(*Im)_2]^+$. Oxidation by an additional electron produces the dication $[(\mu\text{-}N_2)Ru_2^{III/III}DPB(*Im)_2]^{2+}$, which loses dinitrogen. The lability of dinitrogen in the dication complex is predicted from the instability of the analogous ruthenium pentammine complex, $(NH_3)_5RuNNRu(NH_3)_5^{5+}$.[35] On the time scale of the cyclic voltammetric experiment, decomposition (due to ligand exchange disproportionation) of the dicationic bis(five-coordinate) species $[Ru_2^{III/III}DPB(*Im)_2]^{2+}$ similar to that observed for the neutral species does not occur. Reduction of the dication back to the neutral bis(five-coordinate) complex quickly regenerates the dinitrogen complex. Although ligand substitution reactions have not been carried out on the monocation, $[(\mu\text{-}N_2)Ru_2^{II/III}DPB(*Im)_2]^+$, it is expected that this complex is more labile than the neutral complex because the Ru(III) center should have no affinity for dinitrogen thus disrupting the chelate effect of the cofacial diporphyrin. The lability of the monocation is a concern when trying to develop an ammonia oxidation electrode catalyst and will be discussed further in the following paper.[20]

As is the case for $(NH_3)_5RuNNRu(NH_3)_5^{4+}$, it is not possible to reduce the cofacial diporphyrin dinitrogen complex either in the electrochemical experiment or with ordinary reducing reagents (sodium amalgam, zinc amalgam). When the dinitrogen complex is treated with a combination of acid and reducing reagent an uncharacterized insoluble product is formed. Thus far we have been unable to characterize any of the products formed on reaction with acid or with acid in combination with reducing agents.

Conclusions

We have characterized the structure and reactivity of an unusual bridged dinitrogen complex of a metallocofacial diporphyrin. Although the coordination environment between the two porphyrins is unique due to the tether between the porphyrins, the dinitrogen complex is very similar to the untethered $(NH_3)_5RuNNRu(NH_3)_5^{4+}$.

(33) Collman, J. P.; Barnes, C. E.; Swepston, P. N.; Ibers, J. A. *J. Am. Chem. Soc.* **1984**, *106*, 3500–3510.

(34) Guilard, R.; Lopez, M. A.; Tabard, A.; Richard, P.; Lecomte, C.; Brandes, S.; Hutchison, J. E.; Collman, J. P. *J. Am. Chem. Soc.*, in press.

(35) (a) Elson, C. M.; Gulens, J.; Itzkovitch, I. J.; Page, J. A. *J. Chem. Soc. D* **1970**, 875–876. (b) Richardson, D. E.; Sen, J. P.; Buhr, J. D.; Taube, H. *Inorg. Chem.* **1982**, *21*, 3136–3140.

(36) Collman, J. P.; Hutchison, J. E.; Lopez, M. A.; Tabard, A.; Guilard, R.; Seok, W. K.; Ibers, J. A.; L'Her, M. *J. Am. Chem. Soc.*, in press.

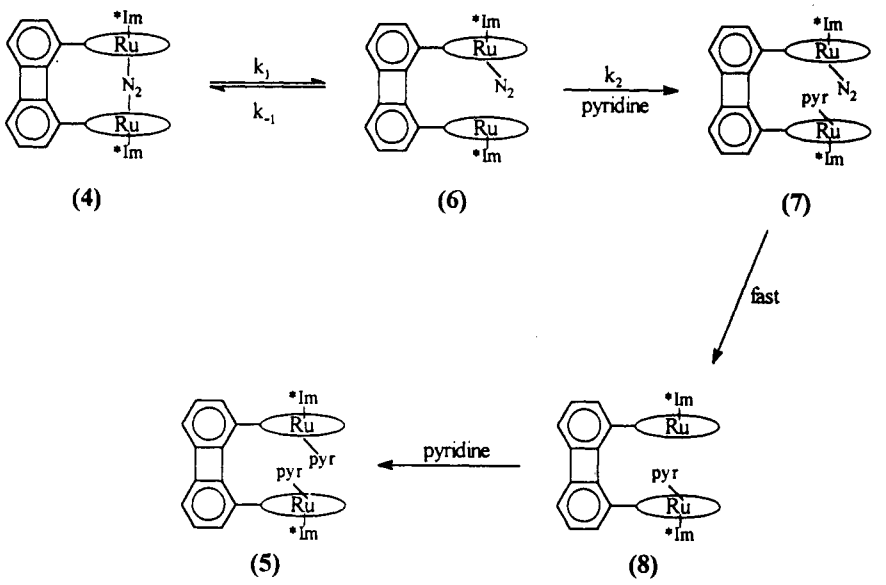

Figure 8. Proposed mechanism for dinitrogen replacement by pyridine for $(\mu\text{-}N_2)Ru_2DPB(*Im)_2$.

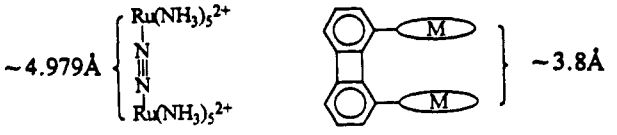

Figure 9. A comparison of the metal–metal distance in the bridged dinitrogen complex $[(NH_3)_5RuNNRu(NH_3)_5]^{4+}$ to the distance between the two metals found in the biphenylene bridged cofacial diporphyrins.[17a,23,36]

There are a number of possible advantages to the tethered cofacial diporphyrin complexes as electrode catalysts for the reduction of dinitrogen: (1) Participation of two metals may facilitate rapid electron transfer to the dinitrogen ligand to a greater degree than monomeric complexes. (2) The cofacial metallodiporphyrins should be robust catalysts because the two metal centers are tethered and will not dissociate upon N–N bond cleavage: a decomposition pathway in reductions of untethered, bridged dinitrogen complexes. (3) Due to the constrained cavity size (Figure 9), the cofacial system might stabilize a transition state along the pathway to a bent reduced nitrogen hydride complex (such as a high energy diazene intermediate) thus promoting the dinitrogen ligand's reactivity with protons. Similar types of geometric distortion have been discussed in the context of transition-state stabilization.[37] Although dinitrogen can be reduced in unstrained systems, we are interested in determining whether the cofacial diporphyrins can induce geometric distortion and thereby increase the reactivity of dinitrogen.

We are currently examining the reactivities of cofacial metallodiporphyrins containing other metals. In particular we are pursuing derivatives involving the earlier transition metals (Mo_2DPB or V_2DPB) which should activate bridged dinitrogen complexes toward protonation and reduction.

Experimental Section

Materials. H_4DPB was prepared using a modified procedure from the literature.[36] Ruthenium dodecacarbonyl (Aldrich) was recrystallized from hexanes prior to use. Tetra-*n*-butylammonium hexafluorophosphate was prepared by mixing equimolar, aqueous solutions of tetra-*n*-butylammonium hydroxide and hexafluorophosphoric acid. The precipitated hexafluorophosphate salt is washed with water, recrystallized twice from ethanol, dried for 2–3 days under vacuum at 100 °C, and immediately taken into the drybox. 1-*tert*-Butyl-5-phenylimidazole was prepared according to the literature procedure.[38] Silica and alumina for use in the drybox were evacuated and dried for 24 h at 1×10^{-2} Torr and 200 °C. Solvents for use in the drybox were distilled from blue or purple sodium benzophenone ketyl solutions (benzene, toluene, hexanes, pyridine, and tetrahydrofuran), from P_2O_5 (dichloromethane), and from $NaOCH_3$ (methanol). Deuterated benzene and pyridine for use as NMR solvents for air-sensitive complexes were stirred as benzophenone ketyl solutions overnight, degassed on a vacuum line (10^{-3} Torr) via five cycles of freeze–pump–thaw, and vapor phase transferred before taking them into the drybox. All other reagents were used as received.

Physical Measurements. ^1H NMR spectra were recorded on either a Nicolet NT-300 or Varian XL-400 Fourier transform spectrometer using benzene-d_6 as solvent and were referenced versus TMS. ^{15}N NMR spectra were obtained in benzene-d_6 on the XL-400 at ambient temperature (unless otherwise stated) employing (^{15}N)-nitrobenzene as an external standard. Electronic absorption spectra were measured on either an HP 8452A or a Cary 219 UV–visible spectrophotometer. Raman spectra were measured in benzene solutions in spinning NMR tubes that were prepared in the drybox and sealed with rubber septa. Mass spectrometry was done at the Mass Spectrometry Facility, University of California, San Francisco.

All electrochemical measurements were made in dichloromethane solutions with tetra-*n*-butylammonium hexafluorophosphate as supporting electrolyte. A 2-mm platinum disk was used as the working electrode. A $Ag/AgNO_3$ pseudo-reference electrode was used and all potentials were measured versus the ferrocene/ferricinium couple by adding ferrocene at the end of each experiment. Potentials are reported vs NHE and were converted to this reference scale by using $E_{1/2}(FeCp_2^{+/0}) = +0.55$ V vs NHE.[39] A special small volume cell[40] was used for all cyclic voltammetric and rotating disk electrochemical experiments. A PAR 173 potentiostat/galvanostat, a PAR 175 universal programmer, and an HP 7046B X-Y recorder were used to make all electrochemical measurements.

Preparation of Compounds. Ru_2DPB (1). This complex was prepared as described by Collman and Kim[15] with some modification in the metalation step. Instead of 2-methoxyethanol, 1,2-dichlorobenzene was used as the solvent and the reaction was carried out under a carbon monoxide atmosphere. The results of these modifications are shorter reaction times and more reproducible yields. Treatment of the reaction mixture with methanol prior to removal of the solvent is crucial to obtaining reproducible, high yields.

Under a carbon monoxide atmosphere, 125 mL of 1,2-dichlorobenzene (degassed by bubbling for 15 min with carbon monoxide) was brought to reflux. At reflux 124 mg (112.2 mmol) of H_4DPB was added followed by 143 mg (223.7 mmol) of ruthenium dodecacarbonyl. Reflux was maintained for 6 h and the reaction followed by TLC (toluene, silica). When the metalation was complete, the reaction mixture was cooled, 20 mL of deaerated methanol was added, and the mixture was stirred another hour. The solvent was removed under vacuum and the crude mixture chromatographed as previously described. Yield: 70%. The

(37) (a) Wolfenden, R. *Acc. Chem. Res.* **1972**, *5*, 10–18. (b) Lienhard, G. E. *Science* **1973**, *180*, 149–154.

(38) van Leusen, A. M.; Schaart, F. J.; van Leusen, D. *Recl. J. R. Neth. Chem. Soc.* **1979**, *98*, 258–262.

(39) Kuwana, T.; Bublitz, D. E.; Hoh, G. *J. Am. Chem. Soc.* **1960**, *82*, 5811–5817.

(40) Le Mest, Y.; L'Her, M.; Collman, J. P.; Kim, K.; Hendricks, N. H.; Helm, S. *J. Electroanal. Chem.* **1987**, *234*, 277–295.

spectroscopic properties have been reported.[15]

$Ru_2DPB(*Im)_2$ (2). Under an argon atmosphere 2 equiv of 1-*tert*-butyl-5-phenylimidazole (92 μL of a 28.3 mM solution in benzene-d_6) were added to a solution of 1.7 mg (1.30 μmol) of Ru_2DPB in 1.0 mL of dry, deaerated benzene-d_6. The ^1H NMR spectrum was recorded immediately. ^1H NMR (C_6D_6, ppm): Porphyrinic resonances: H_{meso} (singlet with an underlying broad resonance, 6 H); biphenylene 6.84 (d, 2 H), 6.63 (dd, 2 H), 6.39 (d, 2 H); $-CH_2CH_3$ 4.12 (m, 8 H), 3.66 (m, 8 H); $-CH_3$ 3.33 (s, 12 H), 3.11 (s, 12 H); $-CH_2CH_3$ 1.60 (t, 12 H), 1.47 (bt, 12 H). Imidazole resonances: *p*-phenyl 6.25 (t, 2 H); *m*-phenyl 6.05 (t, 4 H); *o*-phenyl 4.94 (d, 4 H); $H_{imidazole}$ −0.65 (s, 2 H), −0.76 (s, 2 H); *tert*-butyl −0.94 (s, 18 H).

$Ru_2DPB(*Im)_4$ (3). Under an argon atmosphere 4 equiv of 1-*tert*-butyl-5-phenylimidazole (78 μL of a 39.4 mM solution in toluene-d_8) were added to a solution of 1.0 mg (0.80 μmol) of Ru_2DPB in 1 mL of dry, deaerated benzene-d_6. After 3 h the reaction is complete. ^1H NMR (C_6D_6, ppm): porphyrinic resonances: H_{meso} 9.09 (s, 2 H), 8.96 (s, 4 H); biphenylene (7.4–7.0, obscured by solvent signal); $-CH_2CH_3$ 3.66 (m, 8 H), 3.48 (m, 8 H); $-CH_3$ 3.73 (s, 12 H), 3.15 (s, 12 H); $-CH_2CH_3$ 1.71 (t, 12 H), 1.60 (t, 12 H). Imidazole resonances: 6.65–5.15 (phenyl ring protons); $H_{imidazole}$ 2.19 (s, 2 H), 1.94 (s, 2 H), 1.84 (s, 2 H), fourth $H_{imidazole}$ signal not found; *tert*-butyl −0.36 (s, 18 H), −0.38 (s, 18 H). Mass spectrum: LSIMS(tetraglyme), m/e = 2106, cluster ($[M + H]^+$). Clusters due to loss of one, two, and all four imidazole ligands are also seen.

(μ-N_2)$Ru_2DPB(*Im)_2$ (4). Under a dinitrogen atmosphere, 2 equiv of 1-*tert*-butyl-5-phenylimidazole (284 μL of a 61.4 mM solution in benzene) was added to a solution of 11.4 mg (8.73 μmol) of Ru_2DPB in 2 mL of dry, deaerated benzene. After being stirred for 30 min, the solvent was removed under reduced pressure to yield the dinitrogen complex quantitatively (addition of the ligand to the dimer in the presence of $^{15}N_2$ yields (μ-$^{15}N_2$)$Ru_2DPB(*Im)_2$). Recrystallization of the dinitrogen complex from dichloromethane/methanol produced red crystals that were analytically pure. Calculated for $C_{102}H_{108}N_{14}Ru_2$: C, 70.73; H, 6.28; N, 11.32. Found: C, 70.47; H, 6.20; N, 11.31. ^1H NMR (C_6D_6, ppm): Porphyrinic resonances: H_{meso} 9.02 (s, 4 H), 8.80 (s, 2 H); biphenylene 7.20–7.10 (4 H, obscured by residual solvent peak), 6.90 (t, 2 H); $-CH_2CH_3$ 4.15 (m, 4 H), 3.92 (m, 4 H), 3.42 (m, 8 H); $-CH_3$ 3.48 (s, 12 H), 3.02 (s, 12 H); $-CH_2CH_3$ 1.67 (t, 12 H), 1.58 (t, 12 H). Imidazole resonances: *p*-phenyl 6.26 (t, 2 H); *m*-phenyl 6.04 (t, 4 H); *o*-phenyl 5.04 (d, 4 H); $H_{imidazole}$ 0.48 (s, 2 H), 0.39 (s, 2 H); *tert*-butyl −0.70 (s, 18 H). Mass spectrum: LSIMS (tetraglyme), cluster, m/e = 1733 ($[M + H]^+$). Clusters for loss of one imidazole and for loss of both imidazoles and dinitrogen are also seen. Raman (benzene, 413.13 nm excitation): ν(N–N) of (μ-$^{14}N_2$)$Ru_2DPB(*Im)_2$ = 2112 cm^{-1}, ν(N–N) of (μ-$^{15}N_2$)$Ru_2DPB(*Im)_2$ = 2042 cm^{-1}.

$Ru_2DPB(pyr\text{-}inside)_2(*Im)_2$ (5). To 1.0 mg of (μ-N_2)$Ru_2DPB(*Im)_2$ in 1 mL of toluene was added 1 mL of dry, deaerated pyridine. After the solution was stirred for 2 days, the solvent and excess pyridine were removed under vacuum to quantitatively yield the bis(pyridine) complex. ^1H NMR (C_6D_6, ppm): Porphyrinic resonances: H_{meso} 9.34 (s, 2 H), 8.93 (bs, 4 H); biphenylene 7.11 (d, 2 H), 6.77 (t, 2 H), 6.67 (d, 2 H); $-CH_2CH_3$ 3.76 (m, 8 H), 3.67 (m, 8 H); $-CH_3$ 3.71 (bs, 12 H), 2.93 (s, 12 H); $-CH_2CH_3$ 1.71 (t, 12 H), 1.51 (broad, 12 H). Imidazole resonances: *p*-phenyl 6.52 (t, 2 H); *m*-phenyl 6.34 (t, 4 H); *o*-phenyl 5.60 (d, 4 H); $H_{imidazole}$ 1.96 (s, 2 H), 1.80 (s, 2 H); *tert*-butyl −0.27 (s, 18 H). Pyridine resonances: para 3.41 (t, 2 H), meta 2.57 (t, 4 H), ortho 1.75 (obscured by methyl signal). UV–visible (benzene, nm): 395 (Soret), 501, 527.

Kinetic Measurements. Under a nitrogen or argon atmosphere, 2 mL of a toluene solution containing varying amounts of pyridine were placed in a 1-cm Pyrex cuvette. After the cuvette was sealed with a rubber septum, it was removed from the drybox and placed in the thermostated cell holder of the spectrophotometer. After thermal equilibration for 15 min, a blank spectrum was acquired. Next 25 μL of a 1.37 mM toluene stock solution of the dinitrogen complex was injected through the septum using a gas-tight syringe. The cell was shaken briefly (10 s) and returned to the cell holder and spectra were taken at regular intervals. Observed rate constants were determined by curve fitting absorbance (at 528 nm) vs time data according to the following equation: $Abs(t) = Abs_0 \cdot (\exp(-k_{obs}t)) + Abs_\infty(1 - \exp(-k_{obs}t))$. This analysis yields values for Abs_0, Abs_∞, and k_{obs}. Correlation coefficients for these curves were all between 0.9998 and 0.99998.

Acknowledgment. J.E.H. acknowledges support from the Franklin Veatch Memorial Fellowship Fund, 1987–1989. Support from the National Science Foundation and the National Institutes of Health is acknowledged. We thank the Mass Spectrometry Facility, University of California, San Francisco, supported by the NIH Division of Research Resources (Grant No. RR01614). We thank Dr. Robert A. Reed for obtaining Raman spectra of the dinitrogen complex and Dr. Thomas G. Spiro for the use of the Raman Laboratory at Princeton University which is supported by funds from the U.S. Department of Energy and the National Institutes of Health. The authors thank Dr. Paul Wagenknecht, Dr. Phillip Hampton, and Dr. Erich Uffelman for helpful discussions and Dr. Julie Haack for help in preparing the manuscript.